QCD at LHC : forward physics and UPC collision of heavy ions

Modified jet vertex for the consistent BFKL description of Mueller-Navelet jets

Federico Deganutti **University of Florence**

In collaboration with D. Colferai (INFN)

Trento 26-30 September 2016

BFKL description of Mueller-Navelet jets

Mueller-Navelet jets as preferred testing ground for BFKL dynamics

$$p + p \to jet_1 + jet_2 + X$$

$$X = \text{anything else}$$

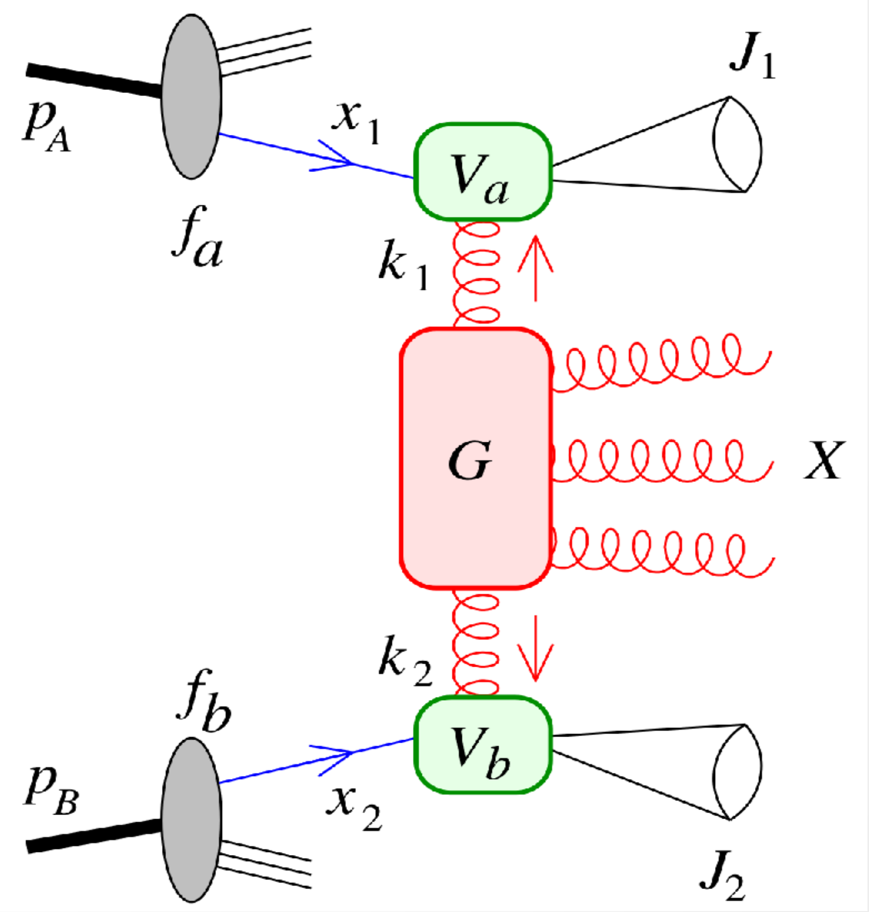

High-energy factorization:

Convolution between BFKL gluon Green function G and the jet vertices $V_{a,b}$

$$\frac{\mathrm{d}\sigma}{\mathrm{d}J_1\mathrm{d}J_2} = \sum_{\mathrm{a,b}} \int_0^1 \mathrm{d}x_1 \mathrm{d}x_2 f_{\mathrm{a}}(x_1) f_{\mathrm{b}}(x_2) \times \int \mathrm{d}^2\mathbf{k}_1 \mathrm{d}^2\mathbf{k}_2 V_a(\mathbf{k}_{J_1}, x_{J_1}, \mathbf{k}_1) G(\mathbf{k}_1, \mathbf{k}_2, \hat{s}) V_b(\mathbf{k}_{J_2}, x_{J_2}, \mathbf{k}_2)$$

- $\mathbf{k}$ = transverse momentum

BFKL description of MN jets at LL

- Gluon Green function

  All order resummation of ladder graphs
- gluon exchange in t-channel
- gluon emission in final state

  Multi-Regge-Kinematics (MRK)

  gluon emission strongly ordered in rapidity

  $$y_1' \gg y_1 \gg \cdots \gg y_n \gg y_2'$$

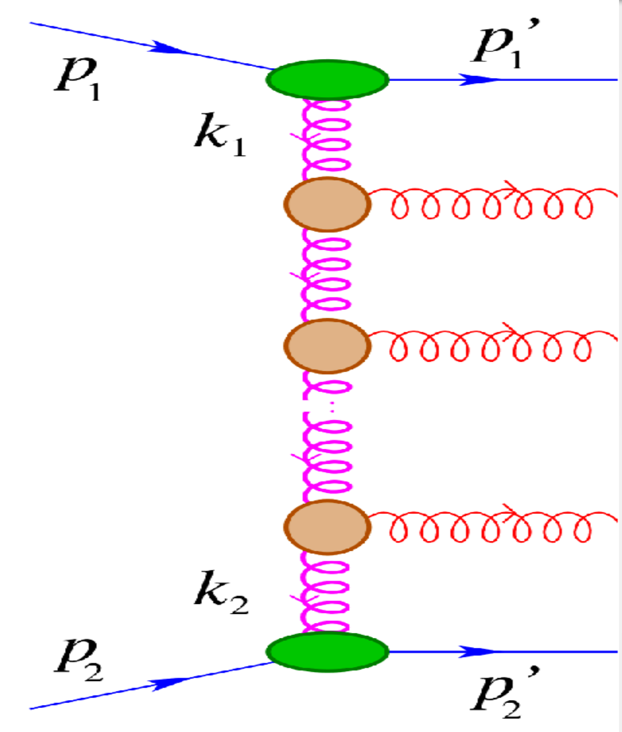

- Jet vertex $\longrightarrow$ tree level

  Only one outgoing parton per vertex

  $$\mathrm{V}_a^{(0)}(\mathbf{k}, x) = \frac{\alpha_s}{\sqrt{2}} \frac{C_{g/q}}{\mathbf{k}^2} S_J^{(1)}(\mathbf{k}; x)$$

  $C_{g/q}$ color factor for incoming gluon/quark

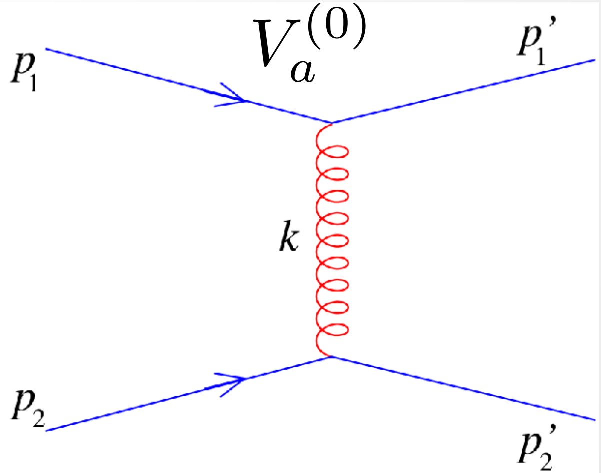

Jet distribution function at LL

$S_J =$ jet distribution function, relates the kinematic variables of the jet identified as MN jet with its partonic constituents

$$\frac{\mathrm{d}\sigma}{\mathrm{d}J_1\mathrm{d}J_2} := \frac{\mathrm{d}\sigma}{\mathrm{d}y_{J_1}\mathrm{d}\mathbf{k}_{J_1}\mathrm{d}y_{J_2}\mathrm{d}\mathbf{k}_{J_2}} := \int \mathrm{d}\sigma S_{J_1} S_{J_2}$$

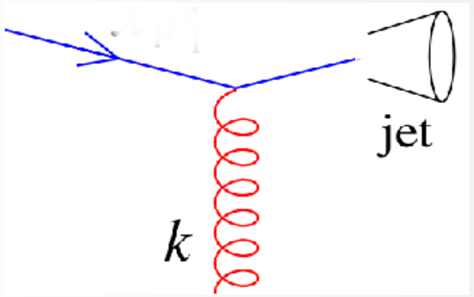

where $S_J = S_J^{(1)} = \delta(y_1' - y_{J_1})\delta(\mathbf{k}_1' - \mathbf{k}_{J_1})$

S_J is the theoretical counterpart of the jet algorithm used in the experimental analysis

For a more faithful jet reconstruction within the perturbative approach a low threshold E_0 is imposed on the jet transverse energy

$\mathbf{k}_J > E_0 = 35\ GeV$ in the CMS analysis

No partons coming from the Green function participate to the MN jets

MRK $\longrightarrow$ vertex partons are the farthest away in rapidity

MN jets at NLL approximation

Gluon Green function

- Higher complexity structure of the contributing Feynman graphs
- Broader kinematic domain

  MRK $\longrightarrow$ Quasi-MRK

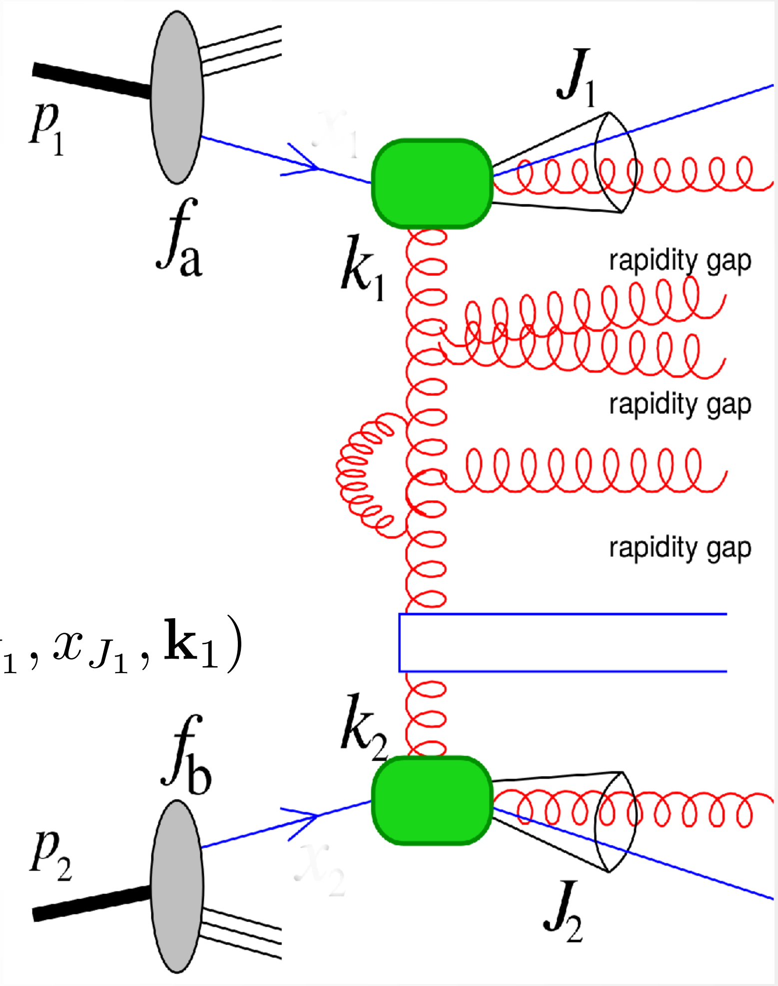

Jet vertex correction $V^{(1)}$

$$V(\mathbf{k}_{J_1}, x_{J_1}, \mathbf{k}_1) = V^{(0)}(\mathbf{k}_{J_1}, x_{J_1}, \mathbf{k}_1) + \alpha_s V^{(1)}(\mathbf{k}_{J_1}, x_{J_1}, \mathbf{k}_1)$$

- Calculated by Bartels, Colferai and Vacca

  for an observable definition not completely consistent with the MN prescription

- QMRK $\longrightarrow$ **two** outgoing partons per vertex

Origin of the inconsistency

Two partons can give rise to one jet in three different ways

1) Composite jet

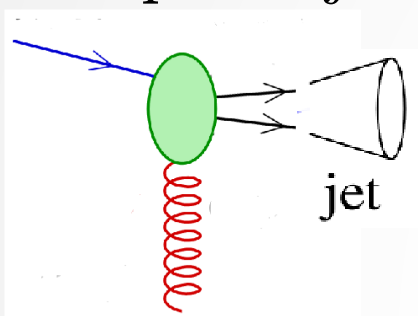

2) Parton 1 is the jet

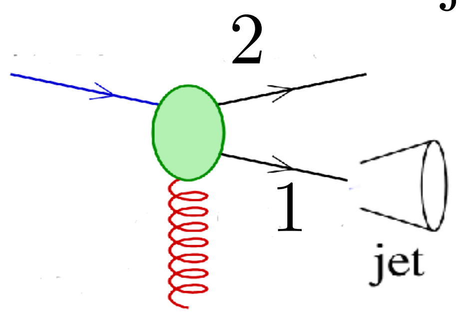

3) Parton 2 is the jet

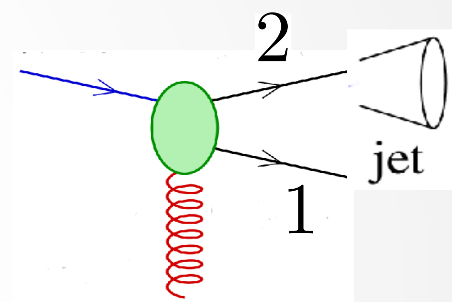

BCV considered an S_J containing all three configuration, even though if e.g. $y_2 > y_1$, case 2) do not select the parton with larger rapidity

Same experimental situation contributes differently to BCV and MN observables

$$Y_i = y_i - y_0$$

$\frac{d\sigma^{(BCV)}}{dY}$ **two** counts Y_1,Y_2

$\frac{d\sigma^{(MN)}}{dY}$ **one** count Y_2

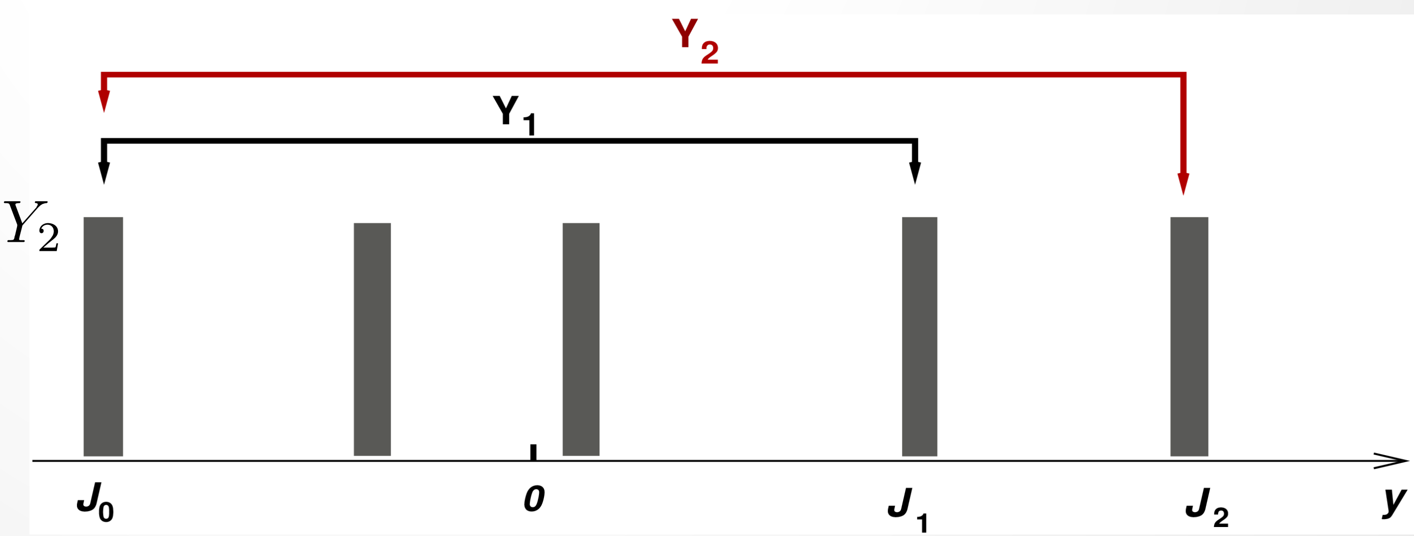

Correction of the inconsistency

$$S_J^{(2)}(\mathbf{k}_1,\mathbf{k}_2,x_1,x_2) = S_J^{(2)}(\mathbf{k}_1+\mathbf{k}_2,x_1+x_2)\Theta(R^2-R_{12}^2)+$$

- Case 2) $\qquad S_J^{(1)}(\mathbf{k}_1,x_1)\Theta(R_{12}^2-R^2)+$
- Case 3) $\qquad S_J^{(1)}(\mathbf{k}_2,x_2)\Theta(R_{12}^2-R^2)$

K_t algorithm: $\quad R_{12}^2 < R^2 := \Delta^2 y_{12} + \Delta^2\phi_{12} < R^2 \;\rightarrow\;$ composite jet

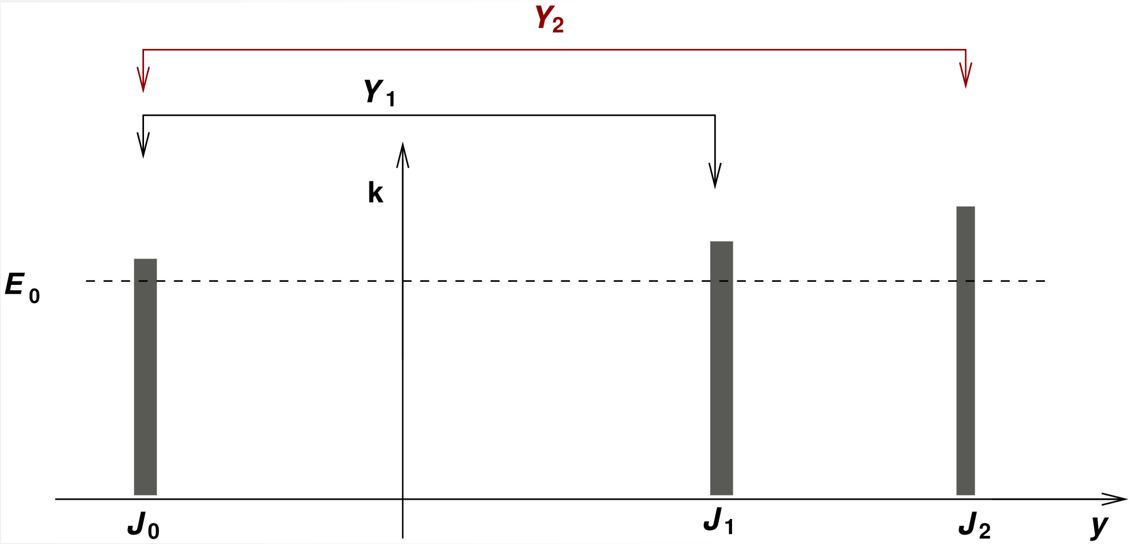

- Partonic configuration

  $|\mathbf{k}_1|, |\mathbf{k}_2| > E_0, \quad y_2 > y_1$

- Case 2) is removed

  $[1-\Theta(|\mathbf{k}_2|-E_0)\Theta(y_2-y_1)] = 0$

- Case 3) is unaltered

  $[1-\Theta(|\mathbf{k}_1|-E_0)\Theta(y_1-y_2)] = 1$

$$S_J^{(2)}(\mathbf{k}_1,\mathbf{k}_2,x_1,x_2) = S_J^{(2)}(\mathbf{k}_1+\mathbf{k}_2,x_1+x_2)\Theta(R^2-R_{12}^2) + 0 +$$
$$S_J^{(1)}(\mathbf{k}_2,x_2)\Theta(R_{12}^2-R^2)$$

- Now only the parton with larger rapidity originate the MN jet

Correction of the inconsistency

$$S_J^{(2)}(\mathbf{k}_1,\mathbf{k}_2,x_1,x_2) = S_J^{(2)}(\mathbf{k}_1+\mathbf{k}_2,x_1+x_2)\Theta(R^2-R_{12}^2)+$$

- Case 2) $S_J^{(1)}(\mathbf{k}_1,x_1)\Theta(R_{12}^2-R^2)\,[1-\Theta(|\mathbf{k}_2|-E_0)\Theta(y_2-y_1)]+$
- Case 3) $S_J^{(1)}(\mathbf{k}_2,x_2)\Theta(R_{12}^2-R^2)\,[1-\Theta(|\mathbf{k}_1|-E_0)\Theta(y_1-y_2)]$

K_t algorithm: $R_{12}^2 < R^2 := \Delta^2 y_{12} + \Delta^2\phi_{12} < R^2 \rightarrow$ composite jet

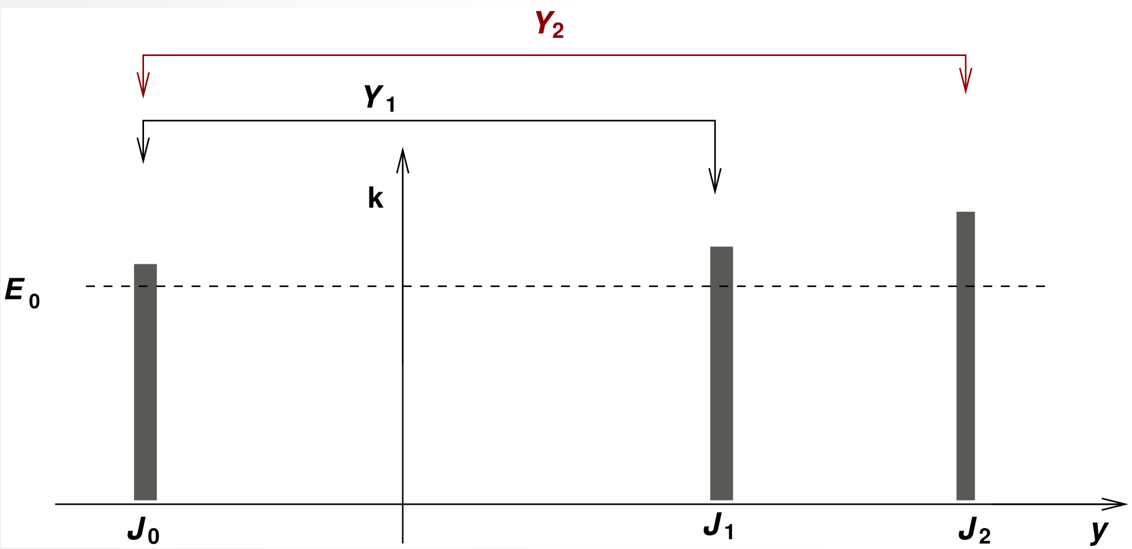

- Partonic configuration
  $|\mathbf{k}_1|, |\mathbf{k}_2| > E_0, \quad y_2 > y_1$
- Case 2) is removed
  $[1-\Theta(|\mathbf{k}_2|-E_0)\Theta(y_2-y_1)] = 0$
- Case 3) is unaltered
  $[1-\Theta(|\mathbf{k}_1|-E_0)\Theta(y_1-y_2)] = 1$

$$S_J^{(2)}(\mathbf{k}_1,\mathbf{k}_2,x_1,x_2) = S_J^{(2)}(\mathbf{k}_1+\mathbf{k}_2,x_1+x_2)\Theta(R^2-R_{12}^2) + 0 + S_J^{(1)}(\mathbf{k}_2,x_2)\Theta(R_{12}^2-R^2)$$

- Now only the parton with larger rapidity originate the MN jet

Correction of the inconsistency

$$S_J^{(2)}(\mathbf{k}_1,\mathbf{k}_2,x_1,x_2) = S_J^{(2)}(\mathbf{k}_1+\mathbf{k}_2,x_1+x_2)\Theta(R^2-R_{12}^2)+$$

- Case 2) $$S_J^{(1)}(\mathbf{k}_1,x_1)\Theta(R_{12}^2-R^2)\,[1-\Theta(|\mathbf{k}_2|-E_0)\Theta(y_2-y_1)]+$$
- Case 3) $$S_J^{(1)}(\mathbf{k}_2,x_2)\Theta(R_{12}^2-R^2)\,[1-\Theta(|\mathbf{k}_1|-E_0)\Theta(y_1-y_2)]$$

If one parton does not have energy above the threshold the correction is not triggered

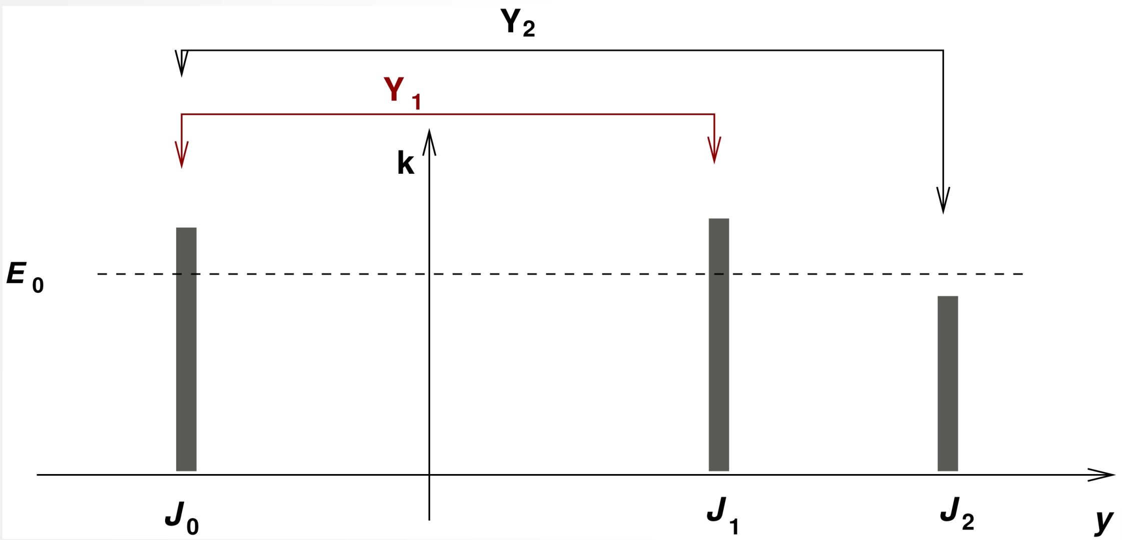

- Partonic configuration

$$|\mathbf{k}_1|>E_0,\ \ |\mathbf{k}_2|<E_0,\ \ y_2>y_1$$

- Both cases unchanged

$$[1-\Theta(|\mathbf{k}_2|-E_0)\Theta(y_2-y_1)]=1$$

$$[1-\Theta(|\mathbf{k}_1|-E_0)\Theta(y_1-y_2)]=1$$

$$S_J^{(2)}(\mathbf{k}_1,\mathbf{k}_2,x_1,x_2) = S_J^{(2)}(\mathbf{k}_1+\mathbf{k}_2,x_1+x_2)\Theta(R^2-R_{12}^2)+$$
$$S_J^{(1)}(\mathbf{k}_1,x_1)\Theta(R_{12}^2-R^2)+S_J^{(1)}(\mathbf{k}_2,x_2)\Theta(R_{12}^2-R^2)$$

- Infrared safety of the parton radiation is preserved

Analysis implementation

- Comparison between the full NLL BFKL prediction for BCV observable definition and the corrected definition
- Observables: $\frac{C_1}{C_0}, \frac{C_2}{C_0}, \frac{C_2}{C_1}, \quad \frac{C_0^{(MN)}}{C_0^{(BCV)}}$, as function of rapidity difference Y between the tagged jets. Where $C_m, m=1,2$ are the first Fourier harmonics of the azimuthal decorrelation:

$$C_m(Y)=\sum_{\mathrm{a,b}}\int_0^1 \mathrm{d}x_1\mathrm{d}x_2 f_{\mathrm{a}}(x_1)f_{\mathrm{b}}(x_2)\int dy_1dy_2\delta(y_1+y_2-Y)\int \mathrm{d}\phi_{J_1}\mathrm{d}\phi_{J_2}\times$$
$$\cos(m(\phi_{J_1}-\phi_{J_2}-\pi))\int \mathrm{d}^2\mathbf{k}_1\mathrm{d}^2\mathbf{k}_2 V_a(\mathbf{k}_{J_1},x_{J_1},\mathbf{k}_1)G(\mathbf{k}_1,\mathbf{k}_2,\hat{s})V_b(\mathbf{k}_{J_2},x_{J_2},\mathbf{k}_2)$$

$$\frac{C_m}{C_0}=\langle cos(m\Delta\phi)\rangle \ , \ C_0=\frac{\mathrm{d}\sigma}{\mathrm{d}Y}$$

Two different kinematic domain:

run 1= $\sqrt{s}=7\ TeV$, run 2= $\sqrt{s}=13\ TeV$

Analysis results

Jet rapidities $|y_{J_i}| < 4.8 \to 0 < Y < 9.6 \to 4 < Y < 9.6$

Jet with fixed transverse energies $|\mathbf{k}_{J_i}| = 35\ GeV$

run 1

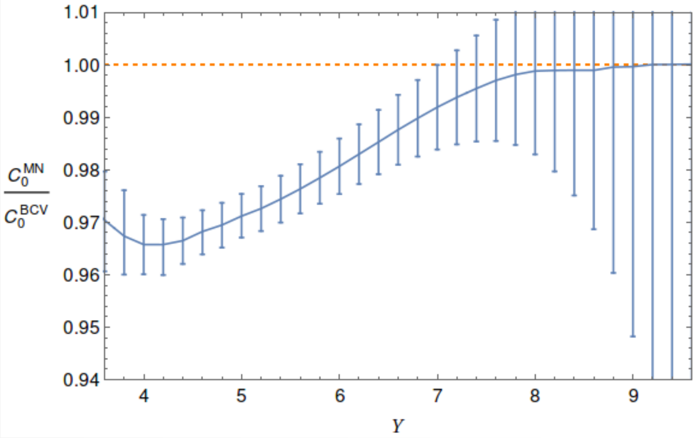

run 2

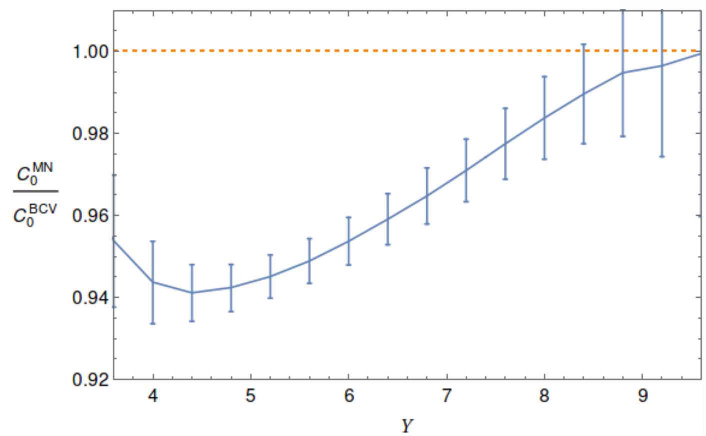

Corrected cross sections show a relative difference of at most 4% run 1, 6% run 2

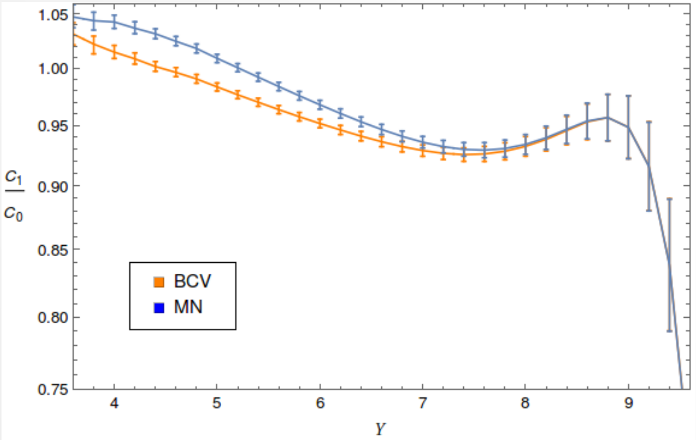

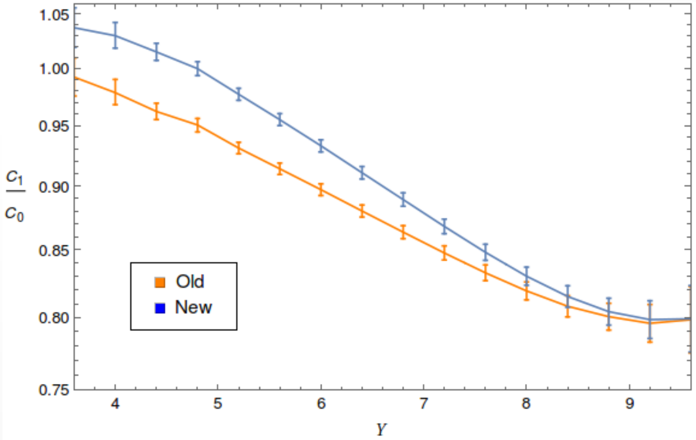

Cosine average greater than 1 for low Y because the density function is not positive definite

- Correction more evident in central rapidity region and for run 2

Analysis results

Jet rapidities $|y_{J_i}| < 4.8 \rightarrow 0 < Y < 9.6 \rightarrow 4 < Y < 9.6$

Jet with fixed transverse energies $|\mathbf{k}_{J_i}| = 35\ GeV$

run 1

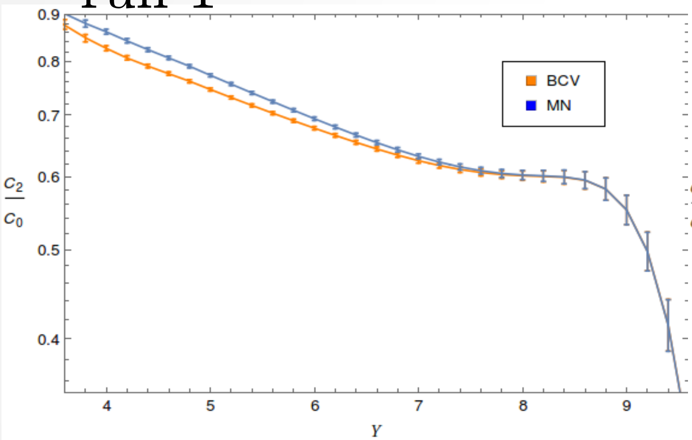

run 2

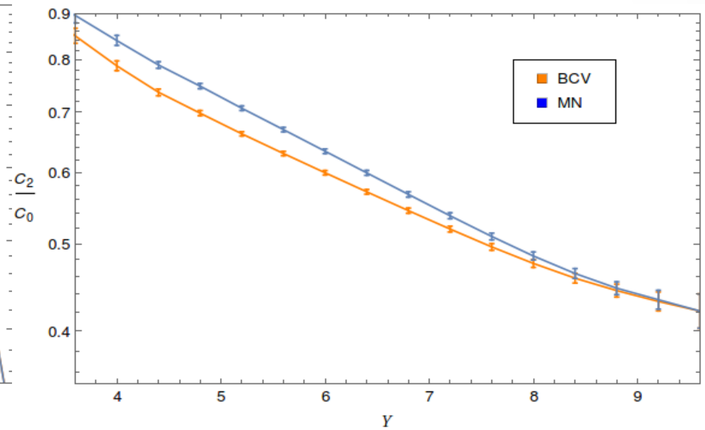

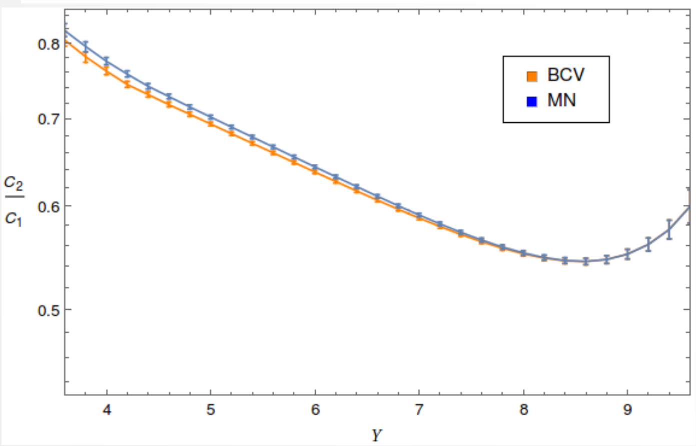

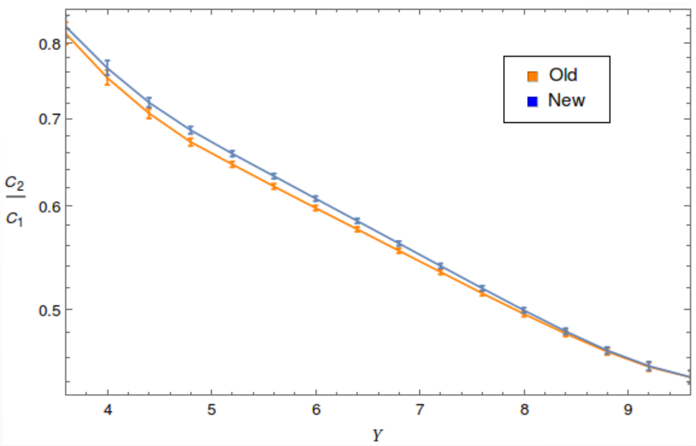

Error bands display the MC error, uncertainties coming from PDFs and renorm/factoriz. scale choice not considered

Correction hardly visible for C_2/C_1, which is the only observable described with satisfactory accuracy by the BFKL approach

Conclusive remarks

- We explored the origin of the inconsistency between the MN observable definition and the definition adopted in the NLL vertex calculation
- We proposed how to resolve the inconsistency
- We assessed the importance of our correction comparing the BFKL predictions at NLL for MN jet production in the BCV and MN observable definition.
- The comparison analysis was repeated for two runs 7, 13 TeV and showed that the relative difference is $\approx 5\%$
- The next step will be to compare the consistent MN description to the CMS data to see whether our correction goes in the direction of a closer reproduction of experimental data. .
- Either way we believe that the implementation of a consistent observable definition alone will not assure a perfect agreement with the experiment.
- Additional ingredients: matching, BFKL hadronization tools..